Elsevier Editorial System(tm) for Electrochimica Acta
Manuscript Draft

Manuscript Number: ITM13-P-27R2

Title: Electrodeposited Cu2ZnSnS4 thin films

Article Type: SI: 13th ISE TM-Pretoria 2013

Keywords: electrodeposition; semiconductors; thin films; CZTS

Corresponding Author: Dr. Marcela Vazquez, PhD

Corresponding Author's Institution: INTEMA

First Author: Matías Valdés

Order of Authors: Matías Valdés; Mmalewane Modibedi; Marcela Vazquez, PhD

Manuscript Region of Origin: ARGENTINA

Abstract: Cu2ZnSnS4 (CZTS) thin films have been prepared using Electrochemical Atomic Layer Deposition (EC-ALD) and also by one-step conventional constant potential electrodeposition. Optimal deposition conditions were investigated using cyclic voltammetry (CV). Then, based on CVs results, CZTS films were grown employing EC-ALD deposition cycles using the sequence Au/S/Cu/S/Zn/S/Sn/S to form the desired quaternary compound. In parallel, conventional one-step electrodeposition was carried out at -0.85 V vs. Ag/AgCl over 1 hour. A thermal treatment in sulfur vapor was also investigated in an attempt to optimize the stoichiometry.
The crystal structure of the films was characterized by XRD and micro Raman spectroscopy, while the morphology, thickness, topography and elemental composition were investigated using FIB-SEM and EDS.

*Response to Reviewers

INTEMA
CONICET
U N M D P

Dr. S. Trasatti
Editor in Chief, Electrochimica Acta
Department of Physical Chemistry & Electrochemistry,
University of Milan,
20133 Milan, Italy,

Dear Sir,

Please find enclosed a revised version of the manuscript "Electrodeposited Cu_2ZnSnS_4 thin films", by M. Valdes, M. Modibedi, M. Mathe, T. Hillie and M. Vazquez

We have modified the figure captions, as required.
I thank you in advance. Sincerely,

Dr. Marcela Vázquez

Av. Juan B. Justo 4302 (B7608FDQ)- Mar del Plata- Argentina- TEL: 54-223-4816600 Int. 241 FAX: 54-223-4810046
e-mail: intema@fi.mdp.edu.ar – www.intema.gov.ar

Electrodeposited Cu_2ZnSnS_4 thin films

M. Valdes[1], M. Modibedi[2], M. Mathe[2], T. Hillie[3], M. Vazquez [1*]

[1]*División Electroquimica y Corrosión, INTEMA, UNMdP-CONICET, J. B. Justo 4302 B7608FDQ Mar del Plata, ARGENTINA*

[2] *Energy Materials, CSIR, Pretoria ZA0001, SOUTH AFRICA*

[3] *National Centre for Nano-structured Materials, CSIR, Pretoria ZA0001, SOUTH AFRICA*

(*) Corresponding author.

Tel.: +54 223 481 6600x244; fax: +54 223 481 0046.

E-mail address: mvazquez@fi.mdp.edu.ar (M. Vázquez)

ISE active member

Abstract

Cu_2ZnSnS_4 (CZTS) thin films have been prepared using Electrochemical Atomic Layer Deposition (EC-ALD) and also by one-step conventional constant potential electrodeposition. Optimal deposition conditions were investigated using cyclic voltammetry (CV). Then, based on CVs results, CZTS films were grown employing EC-ALD deposition cycles using the sequence Au/S/Cu/S/Zn/S/Sn/S to form the desired quaternary compound. In parallel, conventional one-step electrodeposition was carried out at -0.85 V vs. Ag/AgCl over 1 hour. A thermal treatment in sulfur vapor was also investigated in an attempt to optimize the stoichiometry.

The crystal structure of the films was characterized by XRD and micro Raman spectroscopy, while the morphology, thickness, topography and elemental composition were investigated using FIB-SEM and EDS.

Keywords: electrodeposition; semiconductors; thin films; CZTS

1. Introduction

The need to find new materials that can ensure mass production of photovoltaic panels has sparked interest in new alloys and composites. In this scenario, $Cu_2ZnSn(S,Se)_4$ (CZTS) has emerged as a serious substitute for $CuInGa(Se,S)_2$ (CIGSSe), where the indium and gallium are replaced by most abundant elements in the Earth's crust therefore more economical [1]. In particular, CZTS retains the fundamental properties for an ideal absorbent material in solar cells. These include a high absorption coefficient (α ~10^5 cm^{-1}) and direct band gap energy between 1 and 1.5 eV, which matches very well the solar spectrum [2].

Besides the impact that alternative materials can cause, it is important to achieve a real cost reduction. Thus, the techniques used to deposit thin films should involve low costs of equipment, allow depositions in large areas and be easily transferred to industrial scale. Electrodeposition meets all these characteristics and has been used for decades on an industrial scale for coatings with applications in several fields.

Different electroplating routes to obtain CZTS have been reported. So far the most commonly used methodology involves the electroplating of stacked layers of individual elements, followed by treatment in sulfur atmosphere to convert the precursor into CZTS [3-5]. This approach has led to high quality CZTS films yielding efficiencies close to 7% in solar cell devices [5]. Other authors are reported to have chosen to prepare CTZ in a one step electrodeposition [6] or by co-electrodeposition [7] and later incorporated S by sulfurization during annealing.

Some authors have reported a direct electrodeposition of a Cu-Zn-Sn alloy followed by a thermal reaction in sulfur atmosphere [8, 9], while others include a sulfur source in the electrolyte to form a CZTS complete precursor solution [10-12]. The usual complication when using this method is to find a suitable potential window that allows the deposition of all ions in correct proportions, given that reduction potentials are far apart from each other. This can be tackled using complexing ions that shift the reduction potential of the noblest element, approaching it to values close to the more active ones. Citrate ions have been used as complexing agents, as reported by Pawar et al. [10, 13] and thiocyanate ions (CNS^-) by Iljina et al. [14].

Over the last few years, another method for electrodepositing thin films of semiconducting materials has been used with satisfactory results. Electrochemical atomic layer deposition (EC-ALD) is based on atomic layer deposition (ALD). Alternate underpotential deposition (UPD) of the elements in a cycle promotes thin-film formation by deposition of the elements one atomic layer at a time. The method relies on a series of electrochemical surface-limited reactions, which are used to deposit each atomic layer and was originally developed by Stickney and coworkers [15, 16]. Every deposition cycle gives a monolayer of the desired compound, so that the thickness of the film is governed by the number of deposition cycles [17]. The deposition of each individual element can be controlled separately, by carefully choosing conditions such as potentials, electrolyte composition and concentration, pH and deposition times. These conditions have to be adjusted depending on the desired deposit and the substrate being employed. Promising results for EC-ALD for related ternary compounds like $CuInS_2$ [18], $CuInSe_2$ [19, 20] and

$Cu_xSn_yS_z$ [21] have been reported recently. However, the deposition of a quaternary compound is even more challenging.

The purpose of this work is to evaluate diverse electrochemical alternatives to prepare thin films of Cu_2ZnSnS_4, namely EC-ALD and conventional, potentiostatic, one-step electrodeposition.

2. Experimental

2.1. Potentiostatic deposition of Cu_2ZnSnS_4 films

Cu_2ZnSnS_4 (CZTS) films were electrodeposited on top of fluorine-doped tin oxide (FTO, from Pilkington TEC Glass, ~8 Ohms/sq) electrodes (20 x 20 x 3 mm^3). Prior to the deposition, both substrates were cleaned successively in detergent and isopropylic alcohol solution in an ultrasonic bath. A three-electrode cell, with a Pt mesh as counter electrode and a saturated calomel electrode (SCE) as reference electrode, was used. Electrodeposition was carried out employing a PGZ 402 Voltalab® potentiostat/galvanostat. The electrolytic bath consists of an acidic aqueous solution containing 0.02 mol/L $CuCl_2$, 0.015 mol/L $Zn(NO_3)_2$, 0.02 mol/L $SnCl_4$ and 0.02 mol/L $Na_2S_2O_3$. Also, 0.2 mol/L sodium citrate ($Na_3C_6H_5O_7$) was used as complexing agent and the pH was adjusted between 4-4.5 using tartaric acid ($C_4H_6O_6$). CZTS thin films were electrodeposited in potentiostatic mode, applying a potential of -0.85 V vs. SCE (saturated calomel electrode). The deposition time was set at 1 hour and the solution was purged with nitrogen prior to the electrodeposition. After completing the electrodeposition the samples were rinsed with distilled water

and dried in air. The general equation for electrodeposition of CZTS can be described as:

$$2\ Cu^{2+} + Zn^{2+} + Sn^{4+} + 2\ S_2O_3^{2-} + 12\ H^+ + 18\ e^- \rightarrow Cu_2ZnSnS_4 + 6\ H_2O \qquad (1)$$

To improve the crystallinity of the films, thermal treatments were carried out in a three-temperature zone thermal reactor. First, the samples were placed in the cold zone of the tube (room temperature). Then the second zone was heated to 500ºC and in the third zone the sulfur powder (0.3 g) was allowed to reach 300ºC (melting starts at around 200-250ºC). At this point, the samples were moved to the second zone in order to start the sulfurization process, as the vaporized sulfur got in contact with the samples assisted by argon flux. After 1 hour the samples were cooled down by placing them back in the “cold zone”.

2.2 EC-ALD deposition of Cu_2ZnSnS_4 films

The CZTS films were prepared using an automated flow cell electrodeposition system (Electrochemical ALD L.C., Athens, GA). The set-up includes a series of solution reservoirs, pumps and valves, an electrochemical flow cell, a potentiostat, and specialized “Sequencer” software. The reference electrode was Ag/AgCl (3 mol/L KCl) and a gold wire acted as counter electrode. The electrochemical flow cell was designed to promote laminar flow, with the cell volume being 0.3 mL. Solutions were pumped at 50 mL min^{-1}. Pumps and plumbing were contained in a nitrogen purged Plexiglas box. A schematic representation of the equipment is shown in Figure 1.

Substrates used were Au coated glass slides (TA134, 50 Å Ti, 1000 Å Au, EMF Corp., New York). The exposed deposition area is 2.25 cm^2.

Reagent grade chemicals were used to prepare the following electrolytes: 5 10^{-4} mol/L $CuCl_2$, 5 10^{-4} mol/L $ZnSO_4$, 1 10^{-3} mol/L $SnCl_2$ in HCl (pH=1) and 6 10^{-4} mol/L $Na_2S_2O_3$ in 0.1 mol/L KOH. In every case except for $SnCl_2$, 0.1 mol/L Na_2SO_4 was used as supporting electrolyte.

A potential vs. time profile illustrating the EC-ALD cycle chosen to deposit CZTS is shown in Figure 2. UPD potentials for depositing each element were chosen as described below and fixed at the following values, reported against Ag/AgCl: -0.82 V to deposit S, +0.16 V to deposit Cu, -0.75 V to deposit Zn and -0.48 V to deposit Sn. One cycle consisted of letting the solution of each element flow into the cell for 30 s at the potential chosen for the deposition of the corresponding element in the following order:

S/Cu/S/Zn/S/Sn/S/Cu/S/Zn/S/Sn

This process will be referred to as one CZTS EC-ALD cycle, and was repeated 100 times.

2.3. Materials characterization

The crystalline structure of the films was analyzed by X-ray diffraction in grazing incidence configuration (GXRD) using a PANalytical X'Pert PRO diffraction system employing Cu-Kα radiation at 40 kV and 40 mA. The samples were scanned between 15º and 75º, with a step size of 0.01º and with the X-ray beam fixed at 3°. The crystallographic data for each phase were taken from the literature [22].

Raman spectroscopy measurements were performed using an Invia Reflex confocal Raman microprobe using a 50x objective. Excitation was provided with the 514 nm emission line of an Ar^+ laser. In this configuration the laser power on the sample was less than 2 mW measured with a silicon photodiode (Coherent Inc.). For this condition, no thermal effects could be detected as a result of recording the Raman spectra. Raman spectra were taken by averaging 3 acquisitions of 20 seconds each. Raman micro-mapping was performed scanning a square zone (40 x 40 μm) in the sample and recording 25 spectra in the x and y directions. For both axes the step between spectra was set in 20 μm.

The morphology and the chemical composition of the films were registered with a field emission scanning electron microscope (Carl Zeiss Supra 40 FESEM) coupled with an X-ray microanalysis system (Oxford Instrument, INCA processor). Cross-section images of the films were obtained using a Focused-Ion Beam Scanning Electron Microscope (Augira Cobra FIB SEM).

3. Results and Discussion

3.1. Electrodeposition of Cu_2ZnSnS_4 films

Figure 3 presents GXRD diffractograms of electrodeposited samples, before and after the thermal treatment in sulfur. The peaks resulting from FTO (mostly SnO_2) have been identified as F. The pattern also show some peaks that can be attributed to the CuKβ radiation from the X rays that cannot be filtered due to the incidence angle (labeled as β). Further than these, the diffractogram corresponding to the as-deposited sample (Figure 3a) shows peaks that can be

ascribed to binary Cu compounds, mainly Cu_2S and Cu_2O. It is clear that only after annealing can diffraction planes from the CZTS phase be identified in the diffractogram. The major diffraction peaks appear at 2θ = 28.5°, 47.9° and 56.2° attributable to the (112), (220), and (312) crystallographic planes of CZTS. These diffraction planes match the standard XRD pattern of the Cu_2ZnSnS_4 phase (PDF #26-0575). These results are in good agreement with those obtained by Pawar et al. [10, 13], who used a similar precursor bath but employed a Mo-coated substrate and performed the thermal treatment in Ar atmosphere. Similar results have also been shown by Cui et al. [11] and Iljina et al. [14], even when in these cases the annealing treatment was performed in an atmosphere of N_2 + H_2S (5%). Binary secondary phases were detected using both Mo coated glass and ITO as substrates by Cui et al. [11].

Secondary phases are frequently formed during the deposition of CZTS. Even more, in the case of electrodeposited CZTSe, recent mechanistic studies suggested that this compound was formed by reactions among the corresponding binary selenides: Cu_2Se, ZnSe, and $SnSe_2$ [12]. As regards CZTS, the most frequently found byproducts are binary compounds, such as Cu_xS in Cu-rich and ZnS in Zn-rich deposits, as well as ternary phases such as Cu_2SnS_3 and $ZnSnO_3$. However, ZnS with a blend structure (PDF #26-0566), exhibits some planes that are quite close to CZTS (112) and (200) diffraction planes. Thus, Raman spectroscopy is a good complement to XRD and has been successfully used to analyze the structure and the phase purity of CZTS samples [23, 24]. Figure 4 presents Raman spectra of CZTS films, comparing as-deposited and annealed samples. As it can be seen, the spectrum of the as-deposited sample is dominated by bands that can be attributed to binary

phases, mainly SnS_2 and $Cu_{2-x}S$. Again, as in XRD analysis, the presence of CZTS cannot be confirmed, as no band can be ascribed to this quaternary compound. Besides, a couple of bands could not be attributed to any expected byproduct. Instead, after sulfurization there are two signals with peaks at 334 and 286 cm^{-1} that can be related to the two main vibrational modes of kesterite, both with A symmetry [25]. The spectrum in Figure 4 also shows weak contributions at 134, 255 and 362 cm^{-1} that can be attributed to low intensity E and B symmetry modes. After annealing, the spectrum becomes less noisy and exhibits a decrease in the Full Width at Half Maximum (FWHM) of the main bands that can be taken as indicative of an improvement in the crystalline degree of the material.

Raman maps of electrodeposited and annealed films are presented in Figure 5 to show the homogeneity of the composition throughout on the surface. The two main vibrational modes of kesterite with A symmetry (at 334 and 286 cm^{-1}) are always present. This demonstrates that CZTS is evenly distributed along the whole area under analysis. The signal observed around 470 cm^{-1}, originated by $Cu_{2-x}S$, is present with irregular intensity in most of the spectra. In contrast, Raman spectra of annealed films with a monophase composition have been reported by other authors using thiocianate as complexing agents in the precursor bath [14] or an atmosphere of N_2 + H_2S (5%) during annealing [26]. However, in spite of the advantages of Raman spectroscopy mentioned above, there is limited information in the literature of Raman analysis for electrodeposited CZTS. Even in the few cases where the technique is employed, no maps are shown to indicate if the composition and in particular, the absence of binary phases was homogenous along the whole surface.

SEM images showing the morphology of as-deposited and sulfurized CZTS films are presented in Figure 6. As-deposited samples are highly porous and consist of small aggregates. This morphology is very similar to that reported earlier by Jeon et al. [27]. The size of the grains seems to increase after annealing in sulfur, which is consistent with the improvement in the crystalline degree deduced from XRD and Raman results. The grain size of the film after annealing is found to be larger than 1 μm. The morphology of the annealed samples resembles platelets and secondary phases are easy to distinguish. Cui et al. also noted some white spots situated at the surface of an electrodeposited film, and attributed it to Cu_2S crystallites [11].

The chemical composition of the CZTS films before and after the thermal treatments was determined by EDS and is presented in Table 1. It can be observed that the amount of copper in the film decreases while the sulfur content increases with annealing, so that both tend to their respective stoichiometric values. In contrast, the zinc and tin content seems to be much less affected by the sulfurization treatment. Even after annealing in sulfur vapor, the films seem to be slightly deficient in S and comparatively rich in Cu.

3.2. CZTS films deposited by EC-ALD

Cyclic voltammograms were recorded for Au/glass substrates using Cu, S, Sn and Zn precursor solutions, so as to have indicative values for UPD potentials that will be later used to grow the stacks that lead to the quaternary compound. The results obtained for Sn and Cu are shown in Figure 7. Figure 7a is a CV of a clean Au substrate in the Cu^{2+} solution which displays a broad UPD region around 0.16 V, just before with the onset of bulk Cu deposition peak. In the

case of Sn, the UPD region can be seen at around -0.48 V (Figure 7b). The potentials to deposit Zn and S were defined in a similar way (not shown), and resulted to be -0.8 V for Zn and -0.45 V for Sn.

FIB-SEM images were captured to follow the formation of the film and to evaluate the thickness. The a cross-section of a sample deposited using 100 cycles of EC-ALD can be clearly observed in Figure 8(a). The deposit presents some voids but the average thickness can be estimated in 150 nm as shown in Figure 8(b).

The chemical composition of films deposited by EC-ALD was determined by EDS. A typical spectrum is presented in Table 2. It can be seen that all the elements are present in the deposit. EDS maps (not shown) demonstrate that they are evenly distributed along the surface.

XRD/Raman

4. Conclusions

Electrochemical processes, such as conventional electrodeposition and electrochemical atomic layer deposition (EC-ALD) are suitable to produce photovoltaic materials, and present themselves as interesting options that can replace high-vacuum techniques.

Good quality semiconductor thin films can be obtained with one-step electrodeposition as was shown with SEM, XRD and Raman spectroscopy. A post deposition treatment in sulphur atmosphere (thermal annealing) is a key step to improve the properties of the films obtained with one-step electrodeposition. Even if binary undesirable phases appear, they could be etched with a quick immersion in KCN solution.

In the case of EC-ALD, preliminary results show that 100 cycles produce a film of 150 nm of thickness, where EDS analysis shows that all the elements are present. A more exhaustive characterization of the film is currently in progress.

Acknowledgements

This investigation has been supported by CONICET (Consejo Nacional de Investigaciones Científicas y Técnicas, Agencia Nacional de Promoción Científica y Tecnológica), ANCyPT (Agencia Nacional de Promoción Científica y Tecnológica) and Universidad Nacional de Mar del Plata from Argentina.

Also, support from MINCyT (Ministerio de Ciencia, Tecnología e Innovación Productiva) in Argentina and DST (Department of Science and Technology) in South Africa are greatly acknowledged.

Figure captions

Figure 1. Schematic representation of the equipment used to deposit CZTS using EC-ALD

Figure 2. Potential vs. time used to deposit CZTS using EC-ALD.

Figure 3. GXRD patterns of CZTS electrodeposited on FTO at E= -0.85 V during 1 h. a) as-deposited film, dashed line; b) films annealed in sufur, full line. Peaks labeled F denote diffraction planes fron FTO while those labeled β are diffraction planes produced from unfiltered CuK_β radiation. b

Figure 4. Raman spectra of CZTS films electrodeposited on FTO at E= -0.85 V during 1 h for as deposited and annealed samples.

Figure 5. Micro-Raman mapping performed over a 40 x 40 μm region of CZTS films electrodeposited on FTO at E= -0.85 V during 1 h. The sample is later annealed in S vapor.

Figure 6. SEM images (10000 X) of CZTS films (a) as-deposited and (b) after sulfurization.

Figure 7. (a) Cyclic voltammogram in 5.10^{-4} mol/L $CuCl_2$ + 0.1 mol/L Na_2SO_4 for a Au electrode, (b) Cyclic voltammogram in 1.10^{-3} mol/L $SnCl_2$ in HCl (pH=1) Scan rate: 10 mV s^{-1}.

Figure 8. FIB-SEM cross images of CZTS films deposited by EC-ALD (100 cycles). (a) general view; (b) thickness estimation in detailed view.

Figure 9. EDS spectrum of CZTS films deposited by EC-ALD (100 cycles).

References

[1] C. Wadia, A.P. Alivisatos, D.M. Kammen, Materials Availability Expands the Opportunity for Large-Scale Photovoltaics Deployment, Environmental Science & Technology, 43 (2009) 2072-2077.

[2] S. Siebentritt, S. Schorr, Kesterites—a challenging material for solar cells, Progress in Photovoltaics: Research and Applications, 20 (2012) 512-519.

[3] H. Araki, Y. Kubo, A. Mikaduki, K. Jimbo, W.S. Maw, H. Katagiri, M. Yamazaki, K. Oishi, A. Takeuchi, Preparation of Cu_2ZnSnS_4 thin films by sulfurizing electroplated precursors, Solar Energy Materials and Solar Cells, 93 (2009) 996-999.

[4] J.J. Scragg, D.M. Berg, P.J. Dale, A 3.2% efficient Kesterite device from electrodeposited stacked elemental layers, Journal of Electroanalytical Chemistry, 646 (2010) 52-59.

[5] M.-H. Chiang, Y.-S. Fu, C.-H. Shih, C.-C. Kuo, T.-F. Guo, W.-T. Lin, Effects of hydrazine on the solvothermal synthesis of Cu2ZnSnSe4 and Cu2CdSnSe4 nanocrystals for particle-based deposition of films, Thin Solid Films, (2013).

[6] K.V. Gurav, S.M. Pawar, S.W. Shin, M.P. suryawanshi, G.L. Agawane, P.S. Patil, J.-H. Moon, J.H. Yun, J.H. Kim, Electrosynthesis of CZTS films by sulfurization of CZT precursor: Effect of soft annealing treatment, Applied Surface Science, 283 (2013) 74-80.

[7] Y. Wang, J. Ma, P. Liu, Y. Chen, R. Li, J. Gu, J. Lu, S.-e. Yang, X. Gao, Cu2ZnSnS4 films deposited by a co-electrodeposition-annealing route, Materials Letters, 77 (2012) 13-16.

[8] A. Ennaoui, M. Lux-Steiner, A. Weber, D. Abou-Ras, I. Kötschau, H.W. Schock, R. Schurr, A. Hölzing, S. Jost, R. Hock, T. Voß, J. Schulze, A. Kirbs, Cu2ZnSnS4 thin film solar cells from electroplated precursors: Novel low-cost perspective, Thin Solid Films, 517 (2009) 2511-2514.

[9] H. Araki, Y. Kubo, K. Jimbo, W.S. Maw, H. Katagiri, M. Yamazaki, K. Oishi, A. Takeuchi, Preparation of Cu_2ZnSnS_4 thin films by sulfurization of co-electroplated Cu-Zn-Sn precursors, Physica Status Solidi (C) Current Topics in Solid State Physics, 6 (2009) 1266-1268.

[10] S.M. Pawar, B.S. Pawar, A.V. Moholkar, D.S. Choi, J.H. Yun, J.H. Moon, S.S. Kolekar, J.H. Kim, Single step electrosynthesis of Cu2ZnSnS4 (CZTS) thin films for solar cell application, Electrochimica Acta, 55 (2010) 4057-4061.

[11] Y. Cui, S. Zuo, J. Jiang, S. Yuan, J. Chu, Synthesis and characterization of co-electroplated Cu2ZnSnS 4 thin films as potential photovoltaic material, Solar Energy Materials and Solar Cells, 95 (2011) 2136-2140.

[12] W. Septina, S. Ikeda, A. Kyoraiseki, T. Harada, M. Matsumura, Single-step electrodeposition of a microcrystalline Cu 2ZnSnSe4 thin film with a kesterite structure, Electrochimica Acta, 88 (2013) 436-442.

[13] B.S. Pawar, S.M. Pawar, S.W. Shin, D.S. Choi, C.J. Park, S.S. Kolekar, J.H. Kim, Effect of complexing agent on the properties of electrochemically deposited Cu2ZnSnS4 (CZTS) thin films, Applied Surface Science, 257 (2010) 1786-1791.

[14] J. Iljina, R. Zhang, M. Ganchev, T. Raadik, O. Volobujeva, M. Altosaar, R. Traksmaa, E. Mellikov, Formation of Cu2ZnSnS4 absorber layers for solar cells by electrodeposition-annealing route, Thin Solid Films, 537 (2013) 85-89.

[15] B.W. Gregory, J.L. Stickney, Electrochemical atomic layer epitaxy (ECALE), Journal of Electroanalytical Chemistry and Interfacial Electrochemistry, 300 (1991) 543-561.

[16] J.L. Stickney, Electrochemical Atomic Layer Epitaxy (EC-ALE): Nanoscale Control in the Electrodeposition of Compound Semiconductors, in: Advances in Electrochemical Science and Engineering, Volume 7, Wiley-VCH Verlag GmbH, 2001, pp. 1-105.

[17] I. Villegas, J.L. Stickney, Preliminary Studies of GaAs Deposition on Au(100), (110), and (111) Surfaces by Electrochemical Atomic Layer Epitaxy, Journal of The Electrochemical Society, 139 (1992) 686-694.

[18] S. Lin, X. Shi, X. Zhang, H. Kou, C. Wang, Ternary semiconductor compounds CuInS2 (CIS) thin films synthesized by electrochemical atomic layer deposition (EC-ALD), Applied Surface Science, 256 (2010) 4365-4369.

[19] H. Kou, X. Zhang, Y. Jiang, J. Li, S. Yu, Z. Zheng, C. Wang, Electrochemical atomic layer deposition of a CuInSe2 thin film on flexible multi-walled carbon nanotubes/polyimide nanocomposite membrane: Structural and photoelectrical characterizations, Electrochimica Acta, 56 (2011) 5575-5581.

[20] D. Banga, N. Jarayaju, L. Sheridan, Y.-G. Kim, B. Perdue, X. Zhang, Q. Zhang, J. Stickney, Electrodeposition of CuInSe2 (CIS) via Electrochemical Atomic Layer Deposition (E-ALD), Langmuir, 28 (2012) 3024-3031.

[21] F. Di Benedetto, I. Bencistà, S. Caporali, S. Cinotti, A. De Luca, A. Lavacchi, F. Vizza, M. Muniz Miranda, M.L. Foresti, M. Innocenti, Electrodeposition of ternary CuxSnySz thin films for photovoltaic applications, Progress in Photovoltaics: Research and Applications, (2013) n/a-n/a.

[22] International Centre for Difraction Data (ICCD): Powder Difraction File Database, in, Newtown Square, EEUU, 1998.

[23] P.A. Fernandes, P.M.P. Salomé, A.F. Da Cunha, Study of polycrystalline Cu_2ZnSnS_4 films by Raman scattering, Journal of Alloys and Compounds, 509 (2011) 7600-7606.

[24] X. Fontané, V. Izquierdo-Roca, E. Saucedo, S. Schorr, V.O. Yukhymchuk, M.Y. Valakh, A. Pérez-Rodríguez, J.R. Morante, Vibrational properties of stannite and kesterite type compounds: Raman scattering analysis of Cu2(Fe,Zn)SnS4, Journal of Alloys and Compounds, 539 (2012) 190-194.

[25] T. Gürel, C. Sevik, T. ÇağIn, Characterization of vibrational and mechanical properties of quaternary compounds Cu2ZnSnS4 and Cu2ZnSnSe4 in kesterite and stannite structures, Physical Review B - Condensed Matter and Materials Physics, 84 (2011).

[26] S.M. Pawar, B.S. Pawar, K.V. Gurav, D.W. Bae, S.H. Kwon, S.S. Kolekar, J.H. Kim, Fabrication of Cu2ZnSnS4 Thin Film Solar Cell Using Single Step Electrodeposition Method, Japanese Journal of Applied Physics, 51 (2012) 10NC27.

[27] M. Jeon, T. Shimizu, S. Shingubara, Cu2ZnSnS4 thin films and nanowires prepared by different single-step electrodeposition method in quaternary electrolyte, Materials Letters, 65 (2011) 2364-2367.

Table 1

	Cu (at%)	Zn (at%)	Sn (at%)	S (at%)	Cu/(Zn+Sn)	S/(metal)
Stoichiometric	25.0	12.5	12.5	50	1	1
-0.85 V, as-deposited	52.2 ± 4.6	16.2 ± 1.7	7.2 ± 0.8	24.4 ± 1.6	2.2	0.3
-0,85 V, sulfurized	30.6 ± 1.7	15.0 ± 1.4	7.9 ± 2.3	46.5 ± 0.8	1.3	0.9

Table 1. Chemical composition obtained by EDS of different CZTS films. All the films were deposited at 1 hour.

Figure 1

Click here to download high resolution image

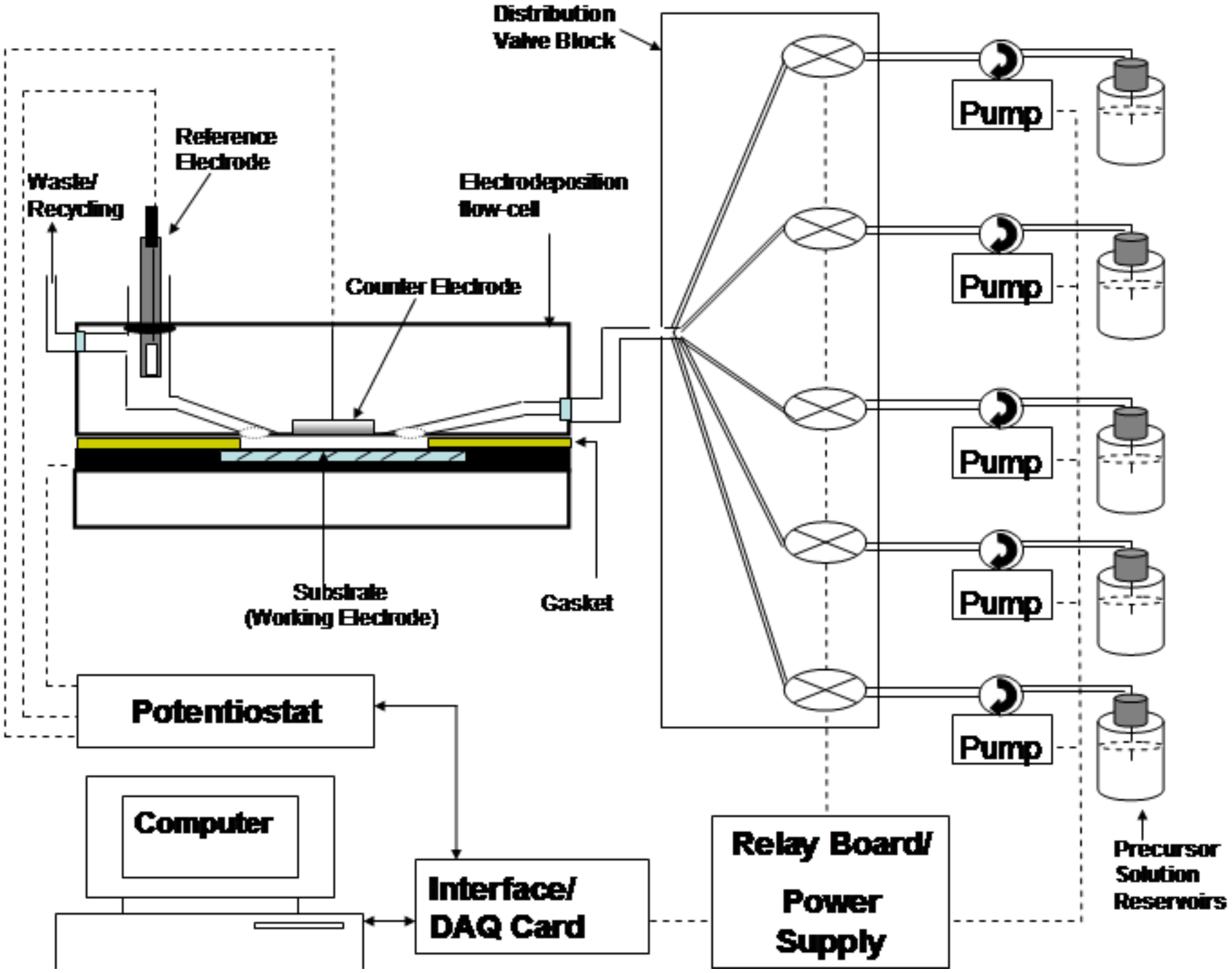

Figure 2

Click here to download high resolution image

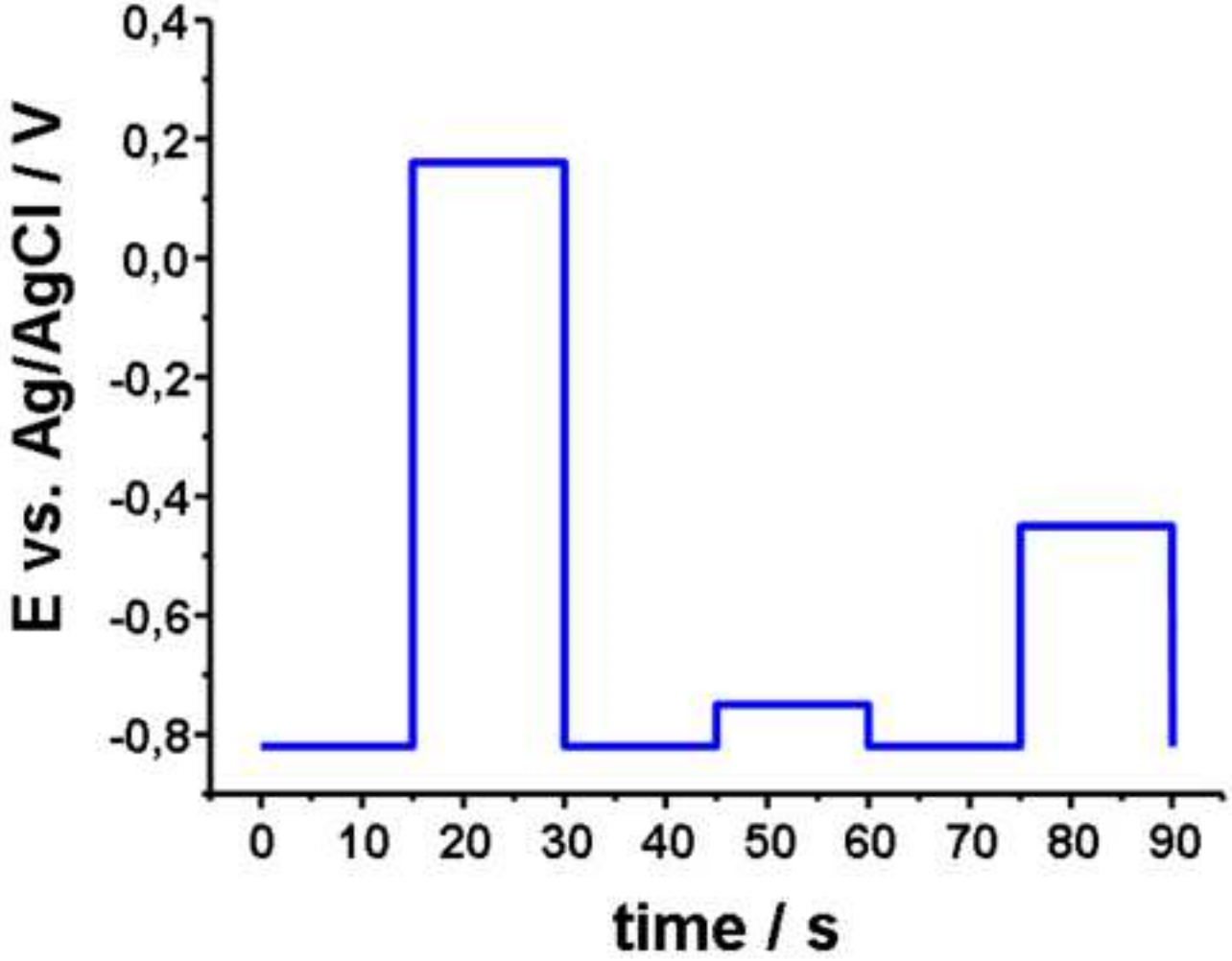

Figure 3a

Click here to download high resolution image

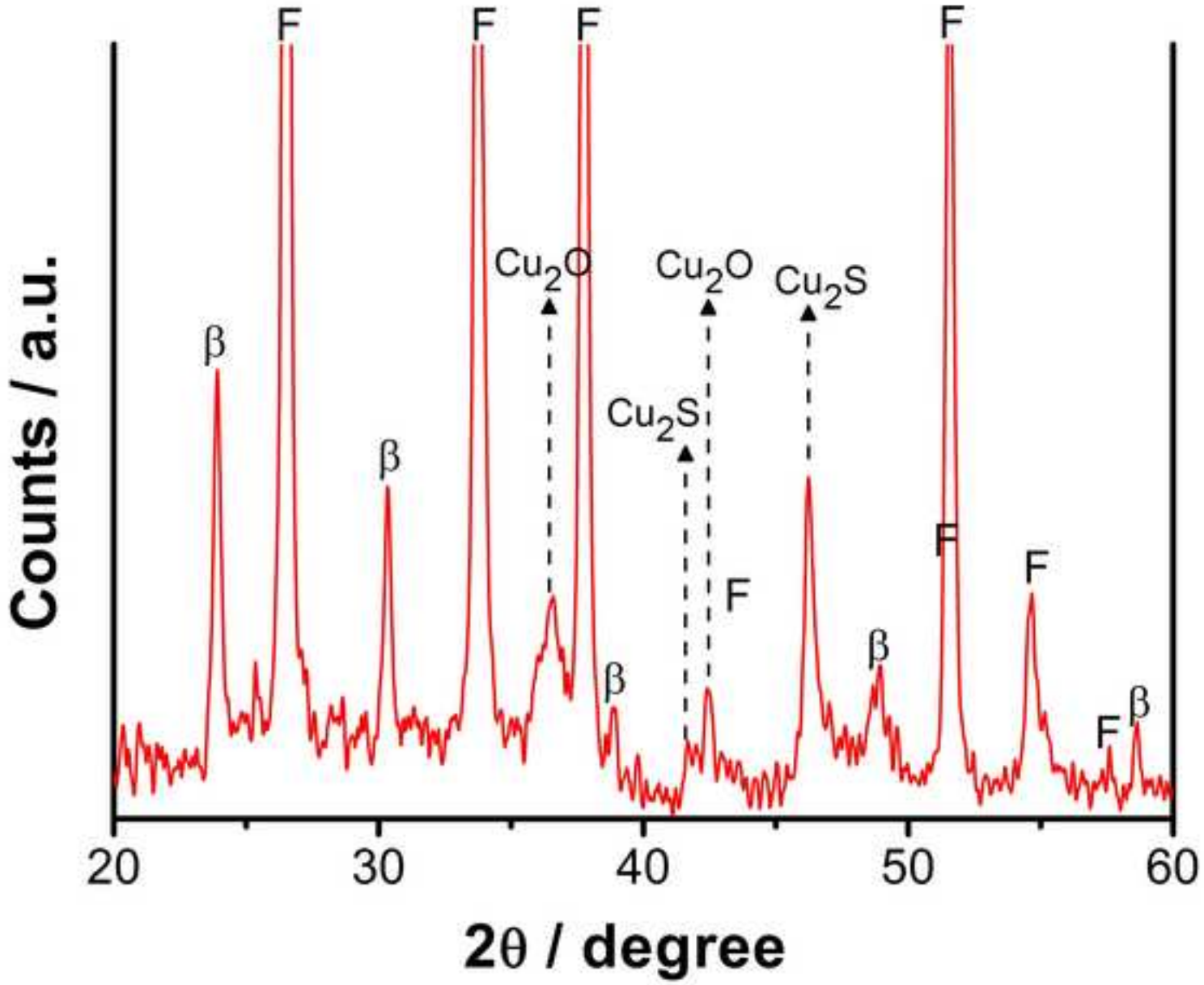

Figure 3b

Click here to download high resolution image

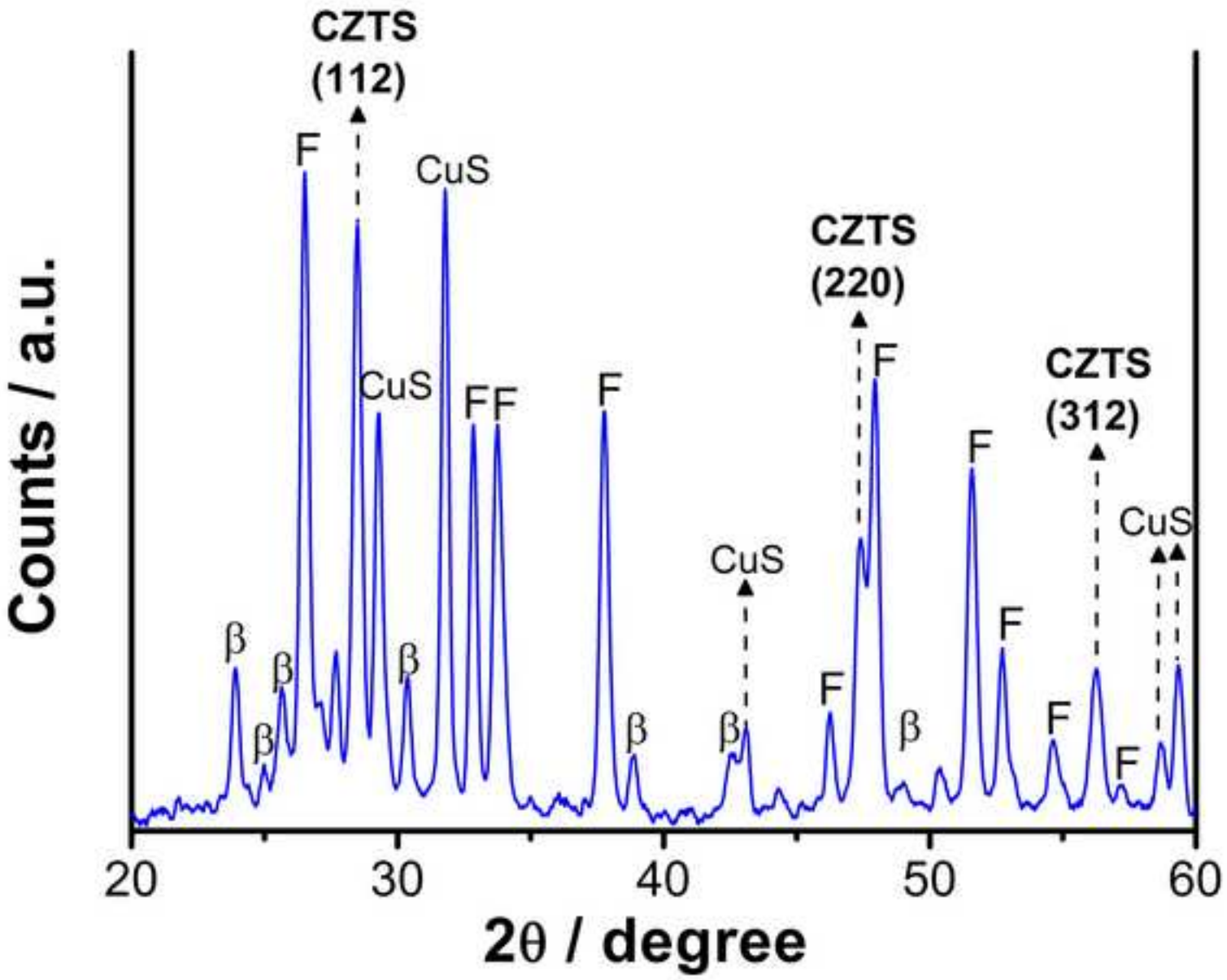

Figure 4

Click here to download high resolution image

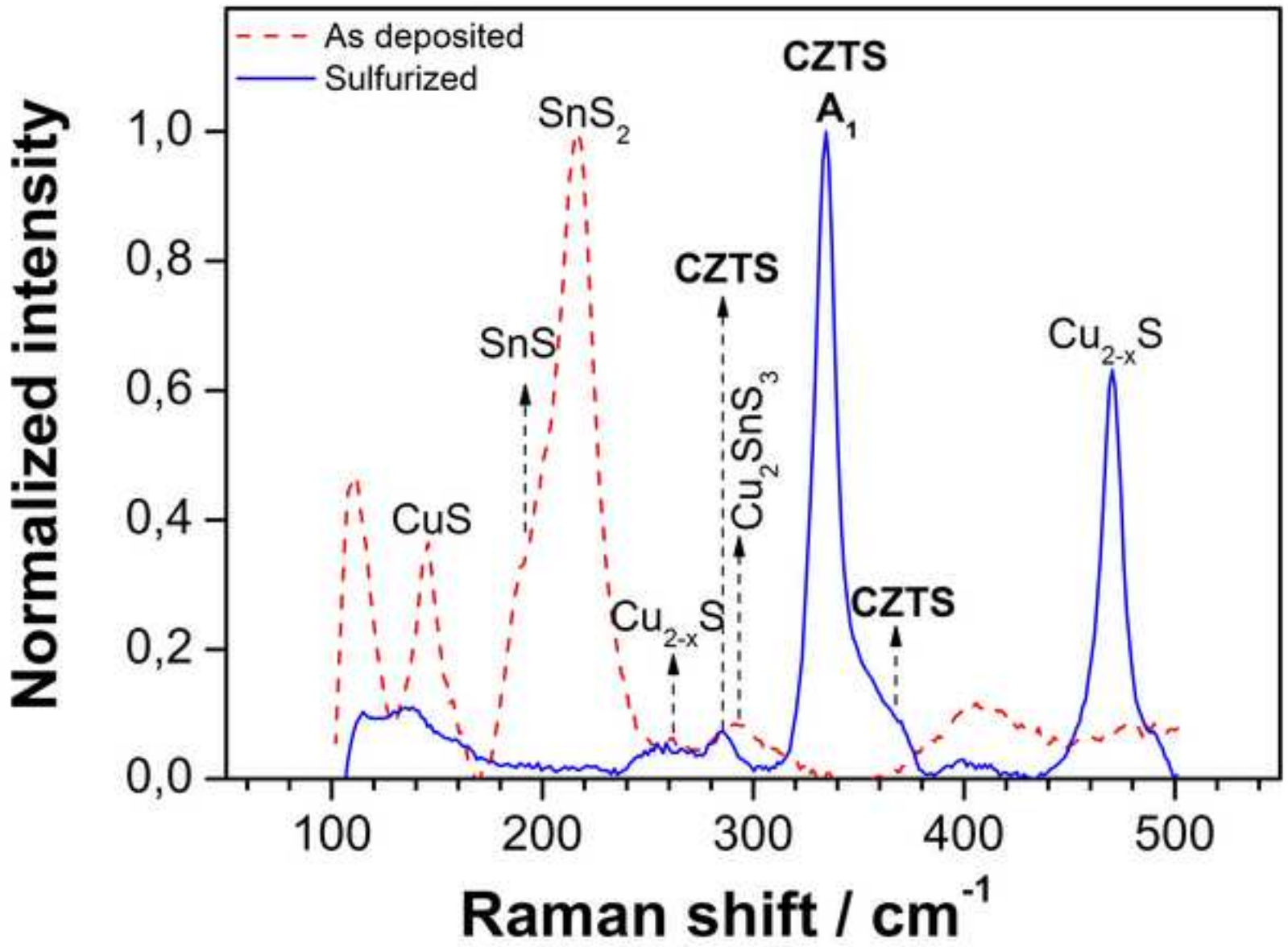

Figure 5

Click here to download high resolution image

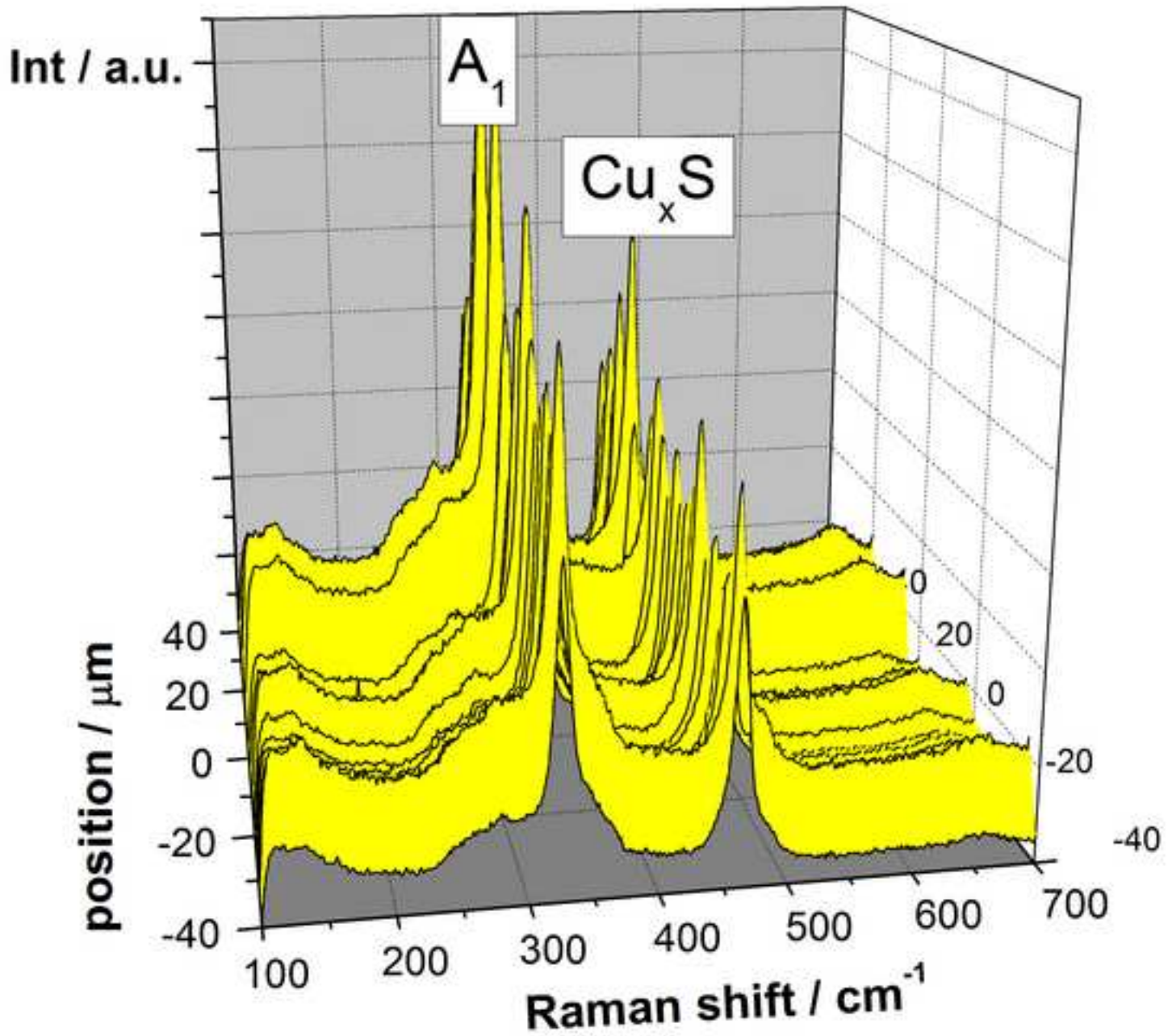

Figure 6

Click here to download high resolution image

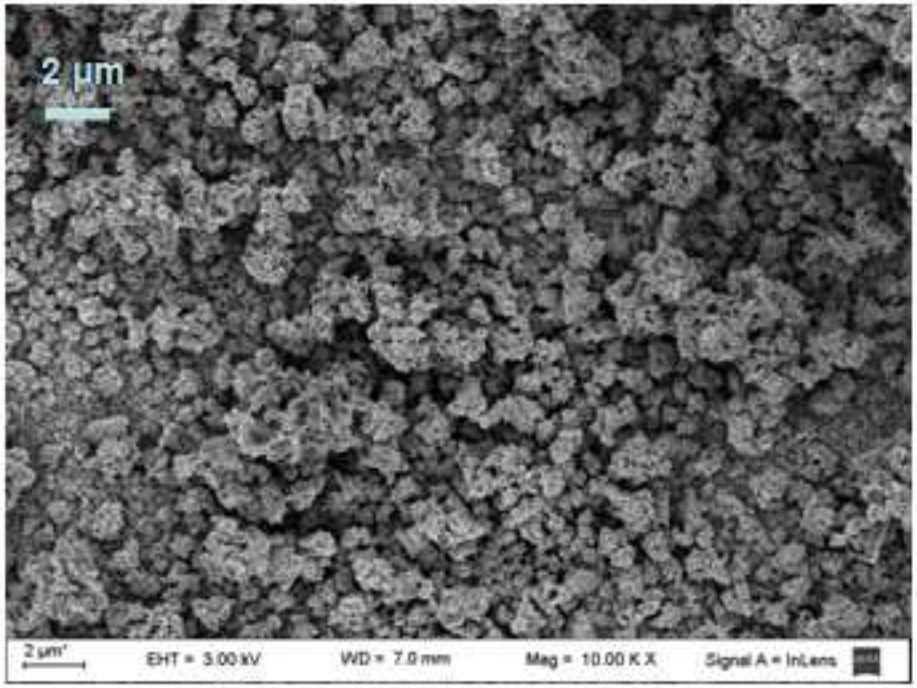

(a)

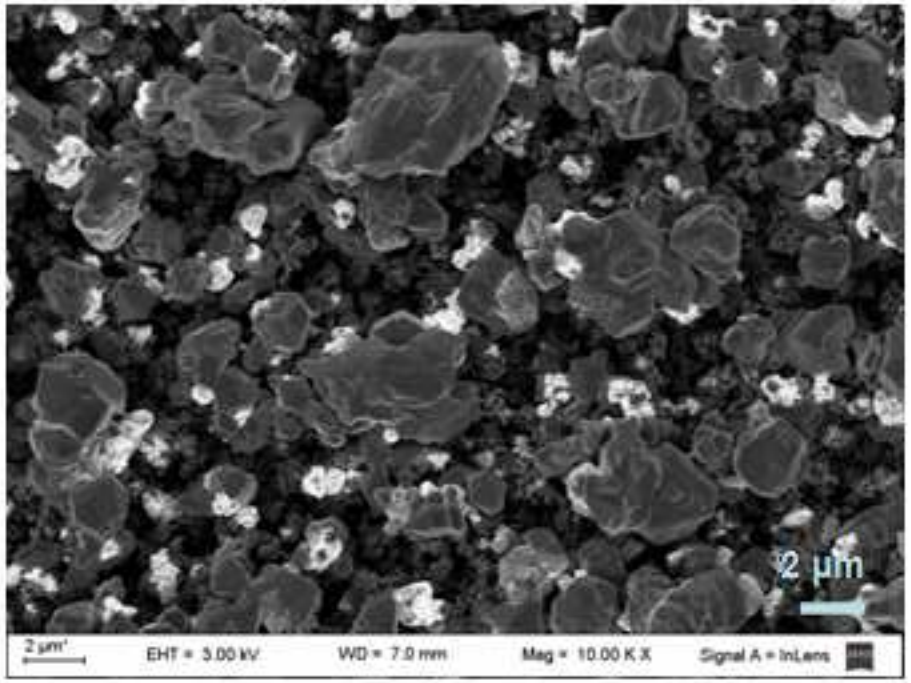

(b)

Figure 7a

Click here to download high resolution image

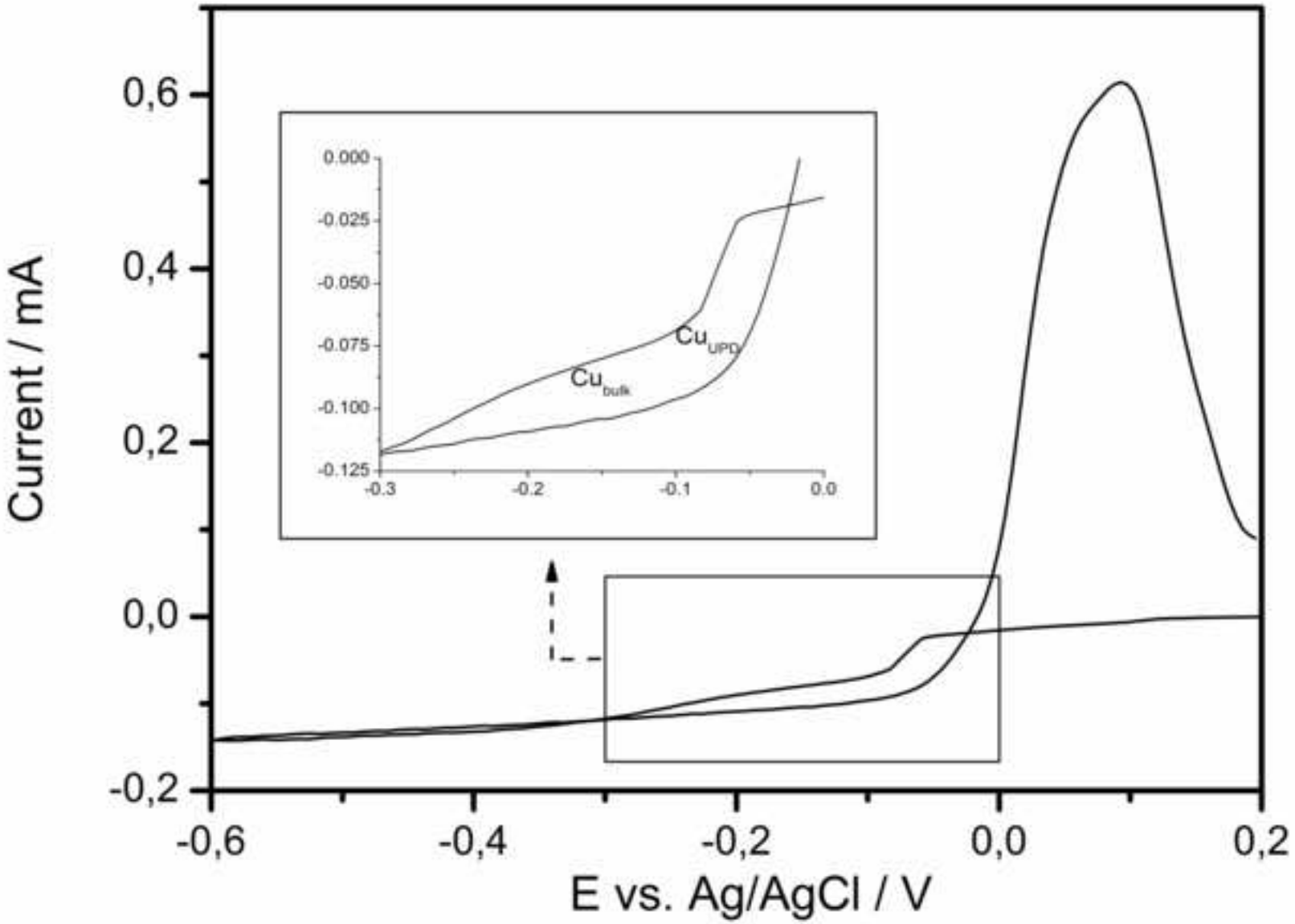

Figure 7b

Click here to download high resolution image

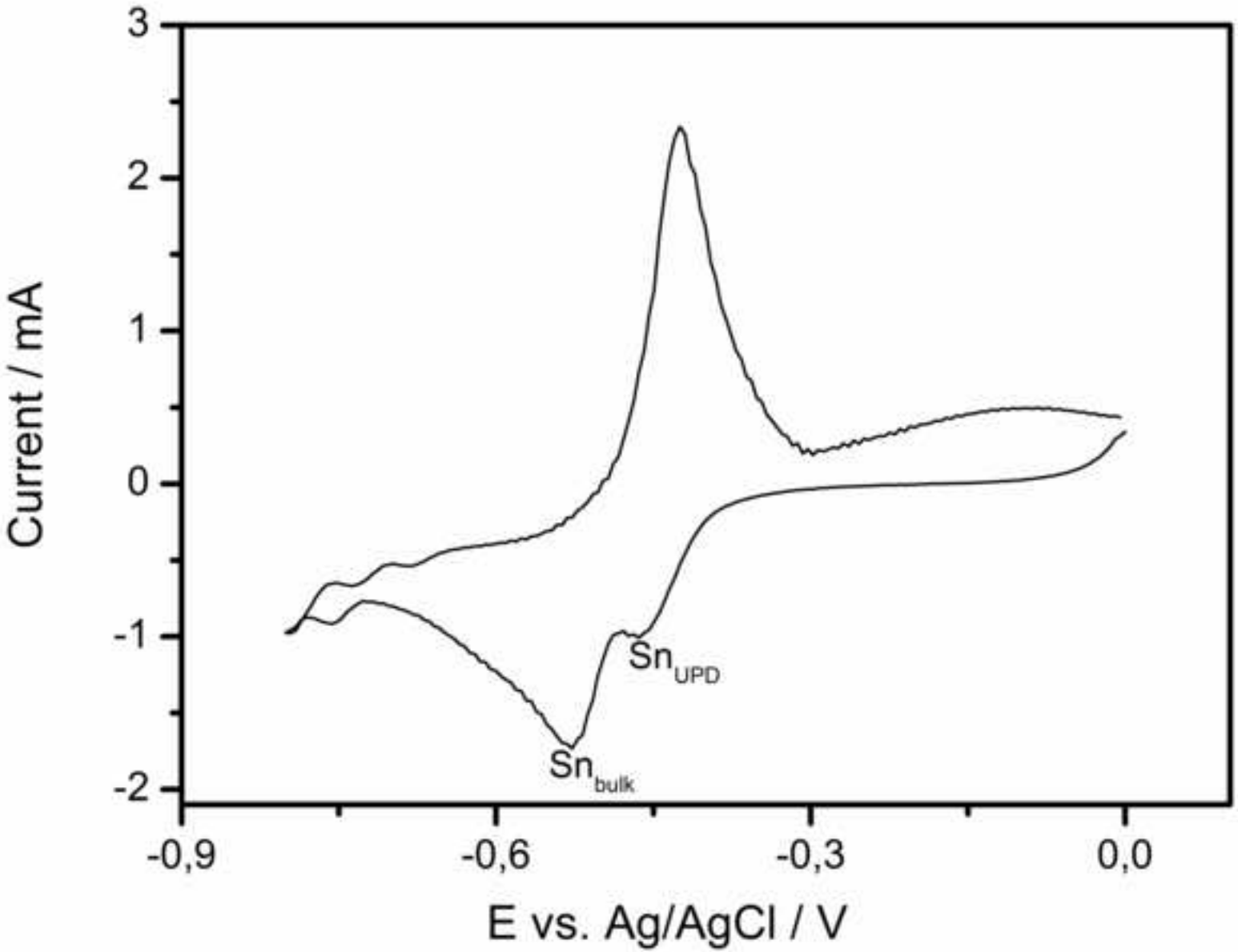

Figure 8a

Click here to download high resolution image

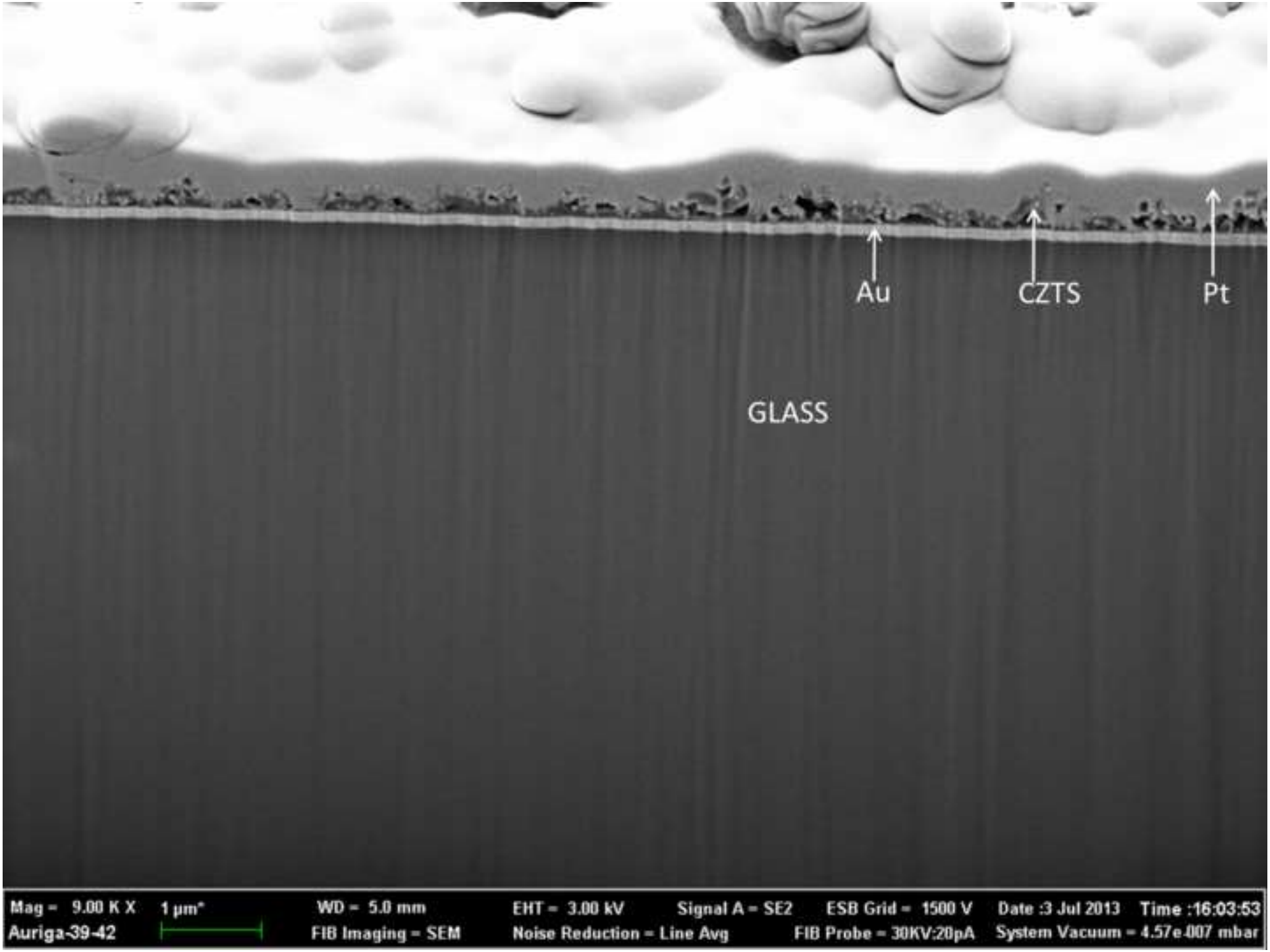

Figure 8b

Click here to download high resolution image

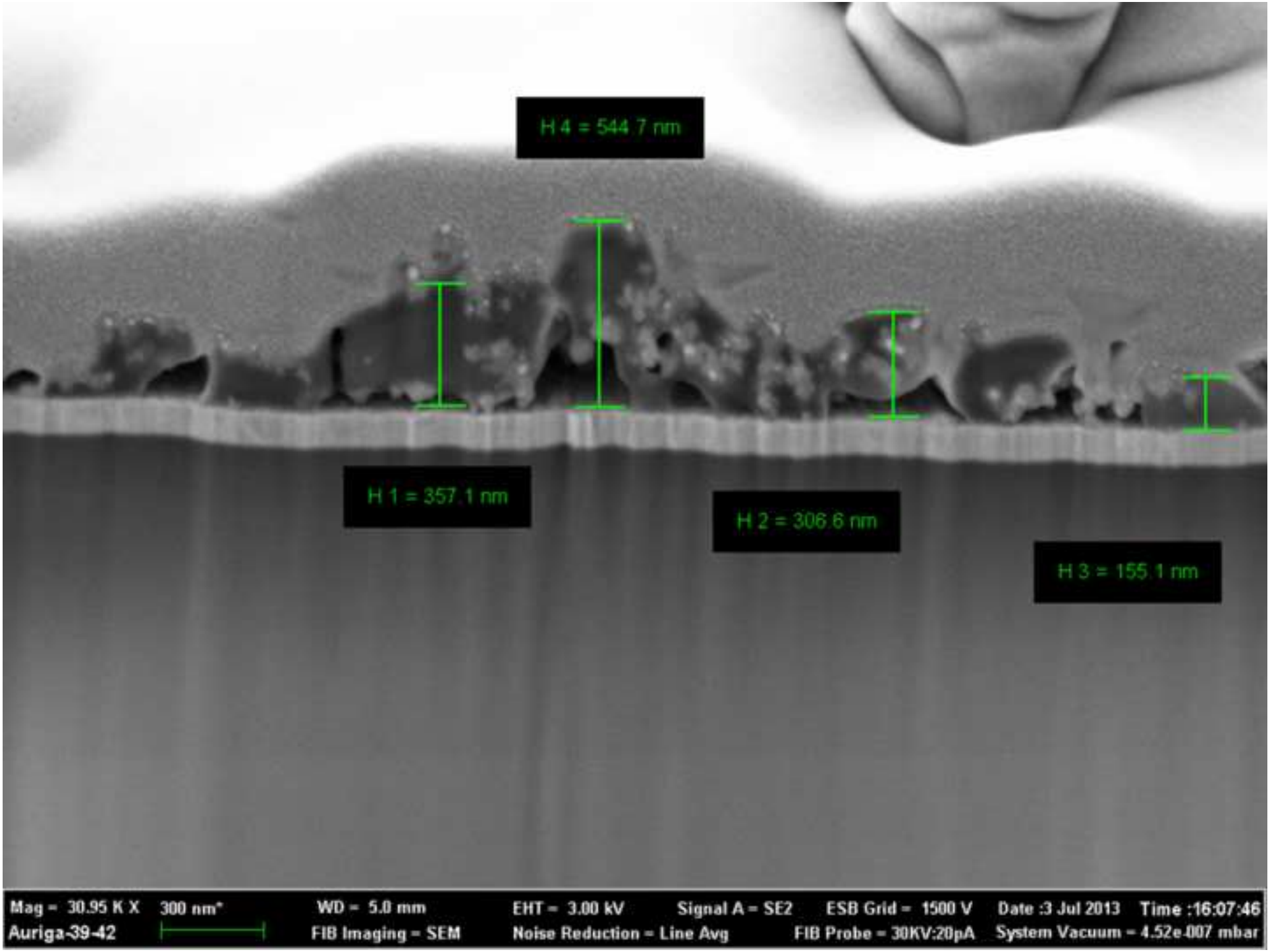

Figure 9

Click here to download high resolution image